

CAVITY FLOW CONTROL OF STEPPED HULL FOR WING-IN-GROUND CRAFT

NZMA Adli¹, MSA Karimi¹, AAT Syahin¹, Z Methal¹, B Bohari^{1,2} and MR Saad^{1,2,3*}

¹Aerospace Research Interest Laboratory (ARIEL), Faculty of Engineering, Universiti Pertahanan Nasional Malaysia, Kem Sungai Besi, 57000 Kuala Lumpur, Malaysia

²Department of Aeronautic Engineering & Aviation, Faculty of Engineering, Universiti Pertahanan Nasional Malaysia, Kem Sungai Besi, 57000 Kuala Lumpur, Malaysia.

³Centre for Defence Research & Technology (CODRAT), Universiti Pertahanan Nasional Malaysia, Kem Sungai Besi, 57000 Kuala Lumpur, Malaysia

Article history

Received

22nd February 2024

Received in revised form

26th May 2024

Accepted

26th May 2024

Published

4th June 2024

*Corresponding author

mohdrashdan@gmail.com

ABSTRACT

A wing-in-ground (WIG) craft is a vehicle that is designed to fly at a low altitude and takes advantage of the ground effect. This helps improve the craft's aerodynamic performance, which in turn reduces fuel consumption as well as improves its overall efficiency. However, the existence of a stepped hull on WIG craft causes an increase in aerodynamic drag during flight. The abrupt geometry of the stepped hull causes flow separation and reduces the craft's aerodynamic performance. Therefore, this study aims to investigate the effect of cavity as passive flow control on the aerodynamic performance of a WIG craft with a stepped hull. The experiments were conducted in a subsonic wind tunnel at a freestream velocity of 5 m/s to 30 m/s. The results show an improvement of up to 7% in the lift-to-drag ratio for the current cavity configurations compared to the baseline model. This shows that the cavity is effective and has a huge potential as a passive flow control for a wing-in-ground craft with a stepped hull.

engine, which is designed to operate in proximity to an underlying surface for efficient utilisation of the ground effect (GE). According to Cui et al. [2], when GE exists, the induced drag is reduced due to the limitations of vertical components of the airflow around the wing tip and the wing tip vortices are disrupted by the ground. Hence, the downwash intensity is reduced, increasing the lift-to-drag ratio. In extreme GE cases, an air cushion is formed due to airflow compression between the surface and the wing, resulting in increased pressure at the pressure surface and decreased pressure at the suction surface. Combining these two effects led to an increase in the lift-to-drag ratio of the WIG craft almost 2 times compared to a light aircraft [2]. Researchers have studied and found that the lift-to-drag ratio increases inversely with the ground height and the maximum lift is found at $0.02 < h/c < 0.03$, where h is the distance from the ground and c is the chord of the wing [3-5]. This is due to the extreme ground effect, where the air between the craft and the surface is compressed, creating an air cushion that allows the craft to hover above it [6].

Since WIG craft are normally designed to take off from large bodies of water, a stepped hull is introduced to improve the craft's hydrodynamics and take-off performance. According to Beng [7], a stepped hull is like a normal hull except with an addition of one or multiple steps to force flow separation and reduce the wetted area, thus reducing the hydrodynamics drag. Saputra [8] proved that the WIG craft with a stepped hull achieved 30 knots (take-off speed) with much less fuel consumption compared to a regular hull. He also found that a stepped hull can reduce the hydrodynamic drag by as much as 8%.

However, while the stepped hull plays a crucial role in improving the craft's take-off performance, the sharp geometry of the stepped hull, similar to a

KEYWORDS

Cavity; Wing-In-Ground Craft; Passive Flow Control; Backwards-Facing Step

INTRODUCTION, LITERATURE REVIEWS

Rozhdestvensky [1] defined a wing-in-ground (WIG) effect vehicle as a heavier-than-air vehicle with an

backwards-facing step (BFS), causes flow separation during the cruise. The flow field of BFS can be divided into four regions, as seen in Figure 1: the separated shear layer, the recirculation region under the shear layer, the reattachment region, and the attached and recovery region [9]. The sudden expansion at the step causes the formation of large vortices behind the step and small vortices at the corner. Chen [9] and Dwarikanath [10] agree that the flow separation near backwards-facing steps could lead to additional drag and noise, contributing to high fuel consumption. Researchers have employed many flow control techniques to improve the overall aerodynamics of the WIG craft and control the flow separation over the backwards-facing steps. For instance, Sujar [11] and Pouryoussefi [12] have conducted studies that employ plasma actuators as an active flow control behind the backwards-facing step. They found that placing the

plasma actuators upstream of the separation point and at the corner of the backward facing steps, reduced reattachment length by as much as 17%. Meanwhile, suction and blowing devices have been experimented with and proven to improve the flow behind the backwards facing step. Khunder [13] finds that using blowing devices improves the pressure coefficient behind the backwards-facing steps as it can delay the flow separation at a small angle of attack ($<10^\circ$). On the other hand, Hahn [14] tested the effect of suction devices slightly upstream of the reattachment point. According to him, the shear layer curves inwards towards the suction point by suction, effectively moving the reattachment point closer to the step wall by as much as 20%. However, suction in this region causes the flow to become unstable. Thus, he proposed using additional suction devices downstream of the separation point [14].

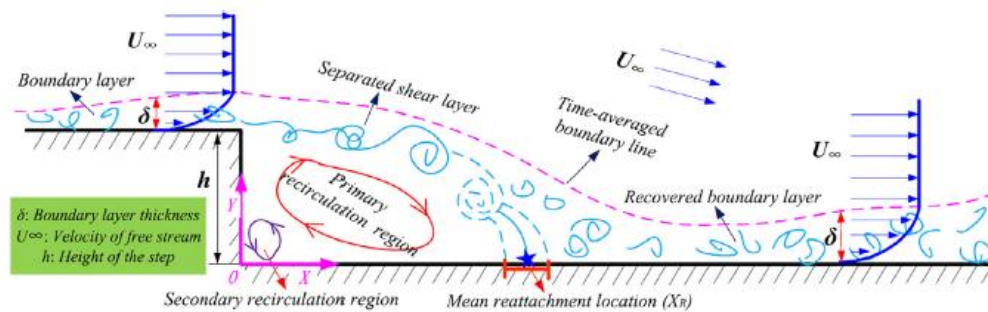


Figure 1: Flow structures behind the backwards-facing step [9]

Researchers have also experimented with using passive flow control behind backwards-facing steps. For instance, Bolgar [15] tested vortex generators in the form of lobes and found a reduced reattachment length of up to 75% for the largest lobe. Methal [16] and Syahin [17] have investigated the use of a micro-ramp vortex generator. In contrast, the usage of a micro-vane vortex generator was studied by Saad et al. [18]. A reduction of up to 21% in drag coefficient, C_D was discovered when using a micro-ramp vortex generator and up to 25% when using a micro-vane vortex generator. Methal [16], stated that this improvement is found because specific configurations can energise the flow effectively making the flow less susceptible to flow separation. Besides, cavities as passive flow control also effectively reduces and increase base pressure and drag depending on their geometry and aspect ratio for sudden expansion flow [19]. Khan [20] tested the effect of a grooved cavity in a convergent-divergent nozzle for subsonic flow and found that the grooved cavity causes an increase in base pressure and decreases depression in the base corner. In his other study, Khan [21] investigated the effect of employing multiple cavities on subsonic flow and found that multiple cavities effectively reduce

base drag by controlling the base pressure. Pandey and Ratakrishnan [22] on the other hand found that the base pressure was strongly affected by multiple aspects of the convergent divergent duct used and the aspect ratio of the cavity. Ratakrishnan [23] finds that increasing the cavity aspect ratio from 2 to 3 decreases the base pressure and further increases from 3 to 4 increases the base pressure. He also agrees with Pandey [24] that introducing secondary vortices by cavity helps smoothen the flow fields. On the other hand, Sethuraman [19] explains that the smaller vortices produced during sudden expansion due to a cavity lead to reduced inflow oscillation. However, at specific flow conditions, the cavity could act as a close surface, rendering the usage of the cavity useless.

A cavity has a vast potential to be used as a passive controller for a wing-in-ground craft with a backwards-facing step. However, most studies employing cavities are conducted in a convergent divergent nozzle and only a few for backwards-facing steps. Thus, this study will focus on experimenting and testing multiple effects cavities such as the cavity configurations, aspect ratios, distances from the backwards facing step and its effectiveness at varying ground clearance.

2. METHODOLOGY

In this study, an experiment using an open loop wind tunnel is conducted to test the effects of multiple aspects of the cavity on the aerodynamic performance of a WIG craft with a stepped hull.

Hull Design and Fabrication

A WIG craft is designed using SOLIDWORKS CAD software. The model is designed based on the 'UH-

18SPW' Hoverwing craft by Universal Hovercraft that is equipped with NACA 4412 airfoils. However, a planning surface and a backwards-facing step are added to simulate the real-life situation of a WIG craft with a stepped hull. A hole or slot is made to change varying cavity types and configurations. Figure 2 shows the dimensions of the stepped hull and Figure 3 shows the CAD model of the modified 'UH-18SPW' Hoverwing craft. The fuselage length is 139 mm with a width of 59.3 mm. The height of the backwards-facing step, h is kept at 5 mm.

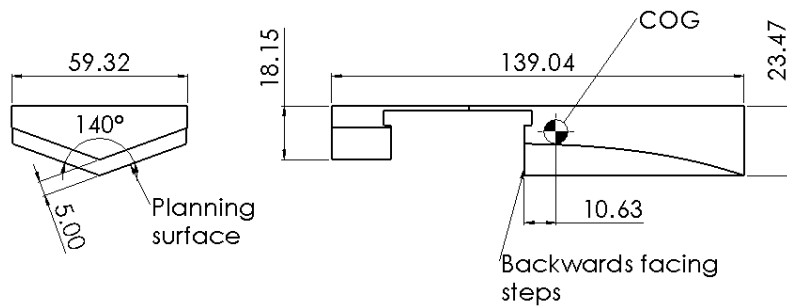


Figure 2: CAD drawing of modified 'UH-18SPW' hull and its dimensions in millimetres (mm)

The WIG model consists of several parts, each part is 3D printed using Ultimaker S2 equipped with PLA filament. Upon completion of 3D printing, the parts are sanded thoroughly using different grades of sandpaper to ensure a smooth and even surface. Then,

the parts are painted with black paint and a lacquer coat to obtain an even smoother surface finish. This is done to avoid any noise in the reading due to rough and uneven surfaces. Finally, the parts are then assembled and glued before testing.

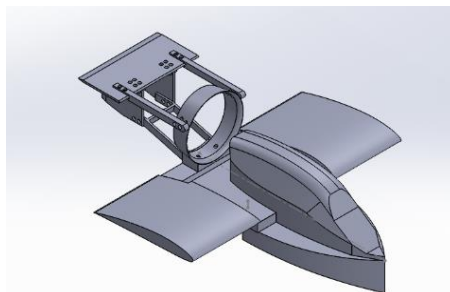


Figure 3: Isometric view of the fully assembled WIG model

Cavity Design and Fabrication

In addition, the cavity's aspect ratio, $AR (W/D)$, and its distance from the backwards-facing step, d is designed based on the step height. The design and dimensions of the cavity are shown in Figure 4. Meanwhile, Figure

5a illustrates the position and measurement of varying parameters in this study where d is the distance of the cavity from the backwards-facing step, W is the width of the cavity, and D is the depth of the cavity, which in this experiment, is fixed at 5 mm equivalent to the height of the backwards facing steps.

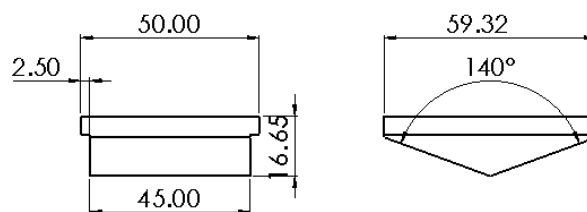


Figure 4: Dimensions of the interchangeable slots in millimetres (mm)

The aspect ratio, AR defined as the width of the cavity, W over its depth, D tested in this experiment are 0.5, 1, 2, 3 and 4. Meanwhile, the distance of the cavity from the backward-facing step, d varied from $0h$ to $5h$. The cavity is also designed with different configurations to find the most suitable type of cavity.

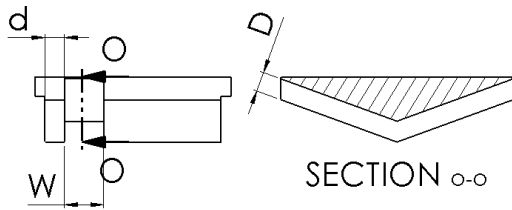


Figure 5a: Position and measurement of varying parameters d , W and D

The configurations tested include closed and open with a fixed aspect ratio and cavity distances. The closed cavity is designed with a ‘side wall’ as shown in Figure 5b. All the configurations, aspect ratio and distance tested are compared with a baseline model with no cavity.

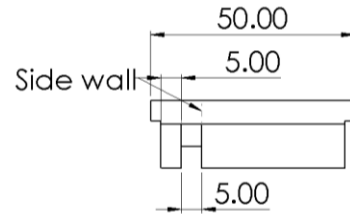


Figure 5b: Position of ‘side wall’ for closed cavity configurations and its dimensions in millimetres (mm)

Figure 5 : CAD drawing and location of sidewall

Wind Tunnel

An open-loop subsonic wind tunnel, Longwin LW-9300R, located in the Faculty of Engineering, National Defence University Malaysia (UPNM) was used to run

the experiments as shown in Figure 6. The wind tunnel can operate from 0 m/s up to 105 m/s and has a test section with dimensions of 0.3 m wide, 0.3 m high and 1 m long.



Figure 6: Longwin LW-9300R wind tunnel

The experiments are conducted at 0° angle of attack and Reynolds number based on step height, Re_h of 1538 to 9225, equivalent to free stream velocity of 5

m/s until 30 m/s. A 3-component force balance is used to measure the value of lift, L and drag, D obtained from the experiments.

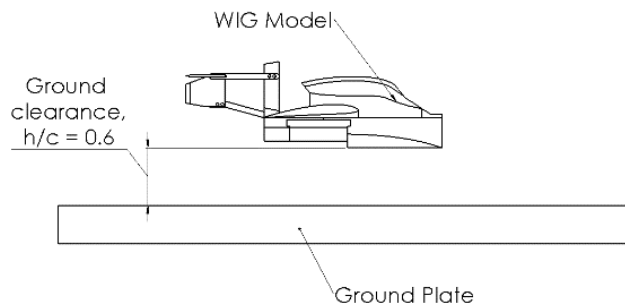


Figure 7: Experimental setup for varying ground heights

The effect of cavity configurations, aspect ratio and cavity distances are tested at a fixed ground clearance,

h/c of 0.6. Then, the best configuration combinations are tested at varying ground clearance of 0, 0.3, 0.6,

0.9 and out of ground, where the craft is no longer under the influence of ground effect. The setup of this experiment is shown in Figure 7 while Figure 8 shows the schematic diagram of the wind tunnel and

experimental setup. As for the case of ‘out of ground’, no ground plate is used to simulate the craft cruising without being under the influence of ground effects.

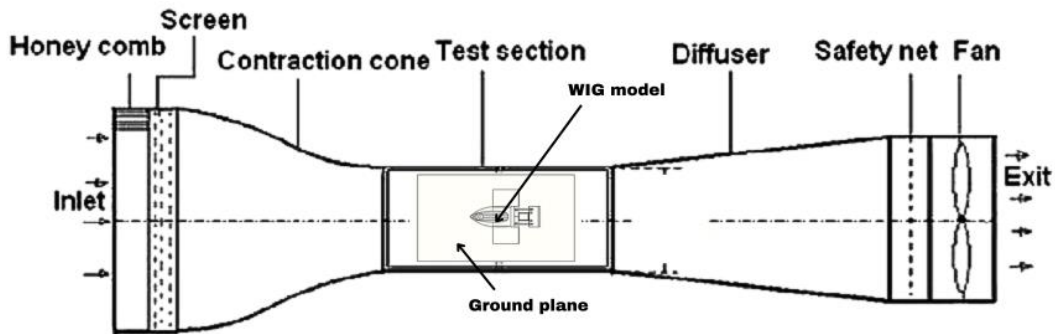


Figure 8: Schematic diagram of experimental setup

To evaluate the aerodynamic performance, the lift and drag obtained from the test are collected and its corresponding lift and drag coefficient are calculated using equations (1) and (2) respectively.

$$C_L = \frac{2F_L}{\rho V^2 S} \quad (1)$$

Where;

- C_L = Lift Coefficient
- F_L = Lift Force
- ρ = Density of Air
- V = Velocity
- S = Surface Area

$$C_D = \frac{2F_D}{\rho V^2 S} \quad (2)$$

Where;

- C_D = Drag Coefficient
- F_D = Drag Force
- ρ = Density of Air
- V = Velocity
- S = Surface Area

On top of that, the Reynolds number based on step height that is used in this experiment is calculated using equation (3).

$$Re_h = \frac{\rho V L}{\mu} \quad (3)$$

Where;

- Re_h = Reynolds Number Based on Step Height
- ρ = Density of Air
- V = Velocity
- L = Height of the Backwards Facing Step
- μ = Kinematic viscosity

3. RESULTS AND DISCUSSION

Effect of Varying Cavity Configuration

In the first experiment, the effects of cavity configurations are tested. Open and closed cavity with the same aspect ratio of 1 is studied under the exact ground clearance, h/c , and Reynolds number. Table 1 shows the parameters used in this experiment.

Table 1: Experimental parameters for varying cavity configurations

Configurations	Open, Closed & Baseline
Aspect Ratio, AR	1
Distance from step, d	1h (5mm)
Ground Clearance, h/c	0.6

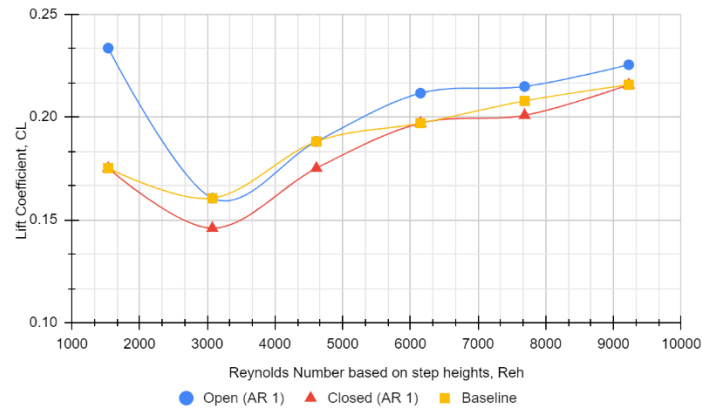


Figure 9: Graph of CL vs. Reh for different cavity configurations

Figure 9 shows the relationship between cavity configurations and the amount of lift produced at different Reynolds numbers. Here, it is observed that from Reynolds number 1000 to 3000, a sudden drop of C_L is observed for all cavity configurations, including the baseline model. Then, until Re 1000, the lift coefficient increases with the Reynolds number until Reynolds number of 9225. From Figure 9 also, we observed that an open cavity has the highest lift

coefficient at almost all Reynolds numbers out of the three configurations tested. Meanwhile, the closed cavity configurations have a comparatively lower lift coefficient, C_L than the baseline model. This shows that the absence of a wall on the side of the cavity plays a crucial role in improving the lift generated. An increase of up to 33% is observed compared to the baseline model.

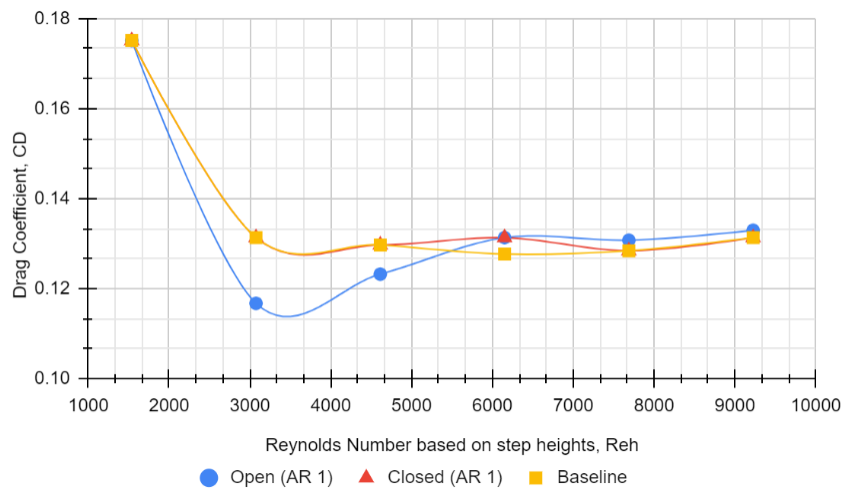


Figure 10: Graph of CD vs. Reh for different cavity configurations

Meanwhile, Figure 10 shows the resulting drag coefficient versus the Reynolds number, Reh . From this figure, it is observed that there is a sudden drop in C_D from Reh of 1000 to 3000. Then, the C_D of all configurations slowly settled at nearly the same value. From Reh 1000 to 6000, we can observe that the open cavity (blue) has the lowest drop in C_D compared to the other configurations. This shows that the open cavity reduces the drag produced due to the

backwards-facing steps at low speeds. On the other hand, in terms of drag coefficient, C_D , the closed cavity performs almost the same as the baseline model for all Reynolds numbers. This indicates that the absence of a wall is the main factor that manipulates the mean flow field behind the backwards-facing steps, thus reducing the drag produced. With the lack of the 'side walls', up to 11% reduction is observed compared to the baseline model.

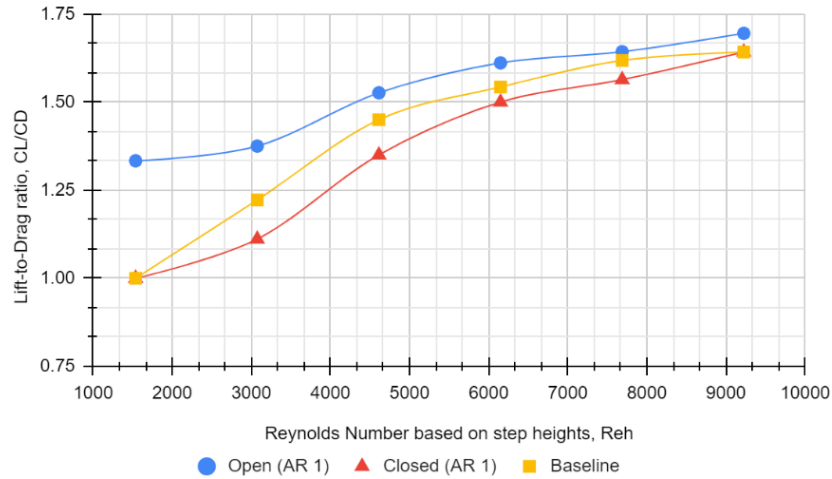


Figure 11: Graph of CL/CD vs. Reh for varying cavity configurations

A graph of lift-to-drag ratio, CL/CD against Reynolds number, Reh is plotted for the cavity configurations of an open cavity (blue), closed cavity (red) and baseline model (yellow). At first glance, it is evident that the open cavity has the highest lift-to-drag ratio out of all configurations tested. Even with the same aspect ratio, the closed cavity performs worse than the baseline for nearly all Reynolds numbers. From Figure 9 and Figure 10 it is clear that although the closed cavity has the same drag coefficient, the reduction in lift produced resulted in a reduction in the lift-to-drag ratio, which shows that the existence of a 'side wall' on the cavity causes a considerable loss in aerodynamic performance shows an open cavity is the best configuration for a WIG craft with a stepped hull. An increase in lift-to-drag ratio of up to 33.3% is observed. These cavity configurations will also be used for the other experiments, which will study the effect of multiple aspects of the cavity more in-depth.

Effect of Varying Cavity Aspect Ratio, AR

For the second experiment, the open cavity configurations with varying aspect ratios are tested and studied to determine the best and the most effective cavity aspect ratio to be used on WIG craft and to be tested in the third experiment. Table 2 shows the parameters used in this experiment.

Table 2: Experimental Parameters for varying cavity's aspect ratio

Configurations	Open
Aspect Ratio, AR	0.5, 1, 2, 3 & 4
Distance from step, d	1h (5mm)
Ground Clearance, h/c	0.6

From Figure 12, we can observe the graph of lift coefficient, CL vs. Reynolds number, and Reh for all the aspect ratios tested and the baseline model. Generally, it is observed that most of the aspect ratio tested performs better in terms of lift coefficient when compared to the baseline model, except for the cavity with an aspect ratio of 0.5. From low to moderate Reynolds numbers, approximately 1000 to 5000, a cavity with an aspect ratio of 2 has the highest lift coefficient compared to the other aspect ratios. However, as the Reynolds number increases, the lift increases drastically for all aspect ratios. This results in the lift coefficient approach and settles at the same value. However, at high speed or high Reh, the aspect ratio of 4, produces the highest lift coefficient. A significant increase of up to 33% compared to the baseline model is observed for this aspect ratio, and an increase of 6.7% is seen at a high Reynolds number, Reh.

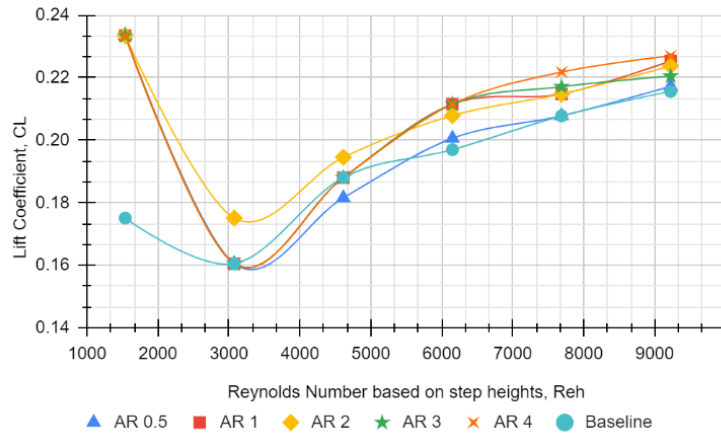


Figure 12: Graph of CL vs. Reh for varying aspect ratio

Meanwhile, Figure 13 shows the graph of drag coefficient versus Reynolds number for all aspect ratios obtained from the second experiment. This figure shows that the cavity with an aspect ratio of 2 has almost the same drag coefficient as the baseline and a higher drag coefficient than the other aspect ratio. Although this cavity significantly improves CL at a low Reynolds number, the resulting CD at the same range of Reynolds number is considerably high compared to the other aspect ratio. Other than that, it is also observed that a cavity with an aspect ratio of 0.5 performs almost similarly to the baseline model in

terms of drag coefficient. Meanwhile, cavities with other aspect ratios, such as 1, 3, and 4, have significantly lower drag coefficients at low to moderate Reynolds numbers. However, at higher Reynolds numbers, approximately 5000, the drag coefficient slowly increases and settles around 0.13 for all cavities, including the baseline model. This shows that while the cavities play an essential role in manipulating the flow field behind the steps, it is also totally dependable on the dimensions of the cavity. Thus, depending on the intentional use, the aspect ratio of the cavity will need to be selected carefully.

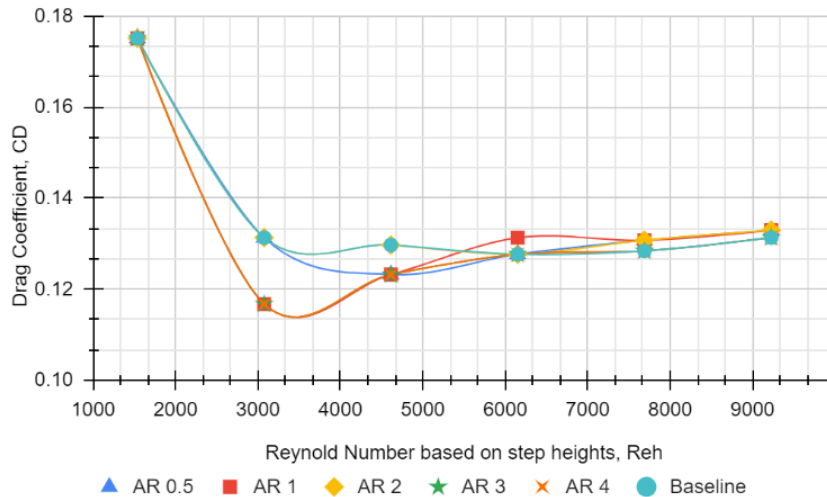


Figure 13: Graph of CD vs. Reh for varying aspect ratio

Figure 14 shows the graph of the lift-to-drag ratio, CL/CD against the Reynolds number, Re, for all aspect ratios tested. This figure shows that a larger aspect ratio contributes to a higher lift-to-drag ratio, which correlates to a higher aerodynamic performance. Generally, almost all aspect ratios of the cavity have a higher aerodynamic efficiency than the baseline model. Only the cavity with an aspect ratio of 0.5 has a nearly identical lift-to-drag ratio compared to the

baseline. This might be the case because, unlike other aspect ratios, the cavity with an aspect ratio of 0.5 has a lower depth of 0.25 m while the others are 0.5 m in depth. This could reduce the effect of a cavity or render the cavity useless. As mentioned by Sethuraman [19], who stated that under certain flow conditions, the cavity could act as a closed surface, thus making the use of the cavity pointless.

From

Figure 14, the cavity with an aspect ratio of 2 has slightly worse aerodynamic performance than the cavity with an aspect ratio of 1 and 3. This behaviour is also observed by Ratakrisnan [22], who found that increasing the cavity aspect ratio from 2 to 3 reduces base pressure. In contrast, a further increase from the aspect ratio of 3 to 4 causes an increase in base pressure. This shows that increasing the cavity's aspect ratio does not necessarily result in an increase in aerodynamic efficiency. On the other hand, the aspect

ratio of the cavity must be selected depending on the flow condition and application. On the other hand, from

Figure 14 also, we can observe that from Reynolds number of 1000 to 6000, cavity with aspect ratios of 3 and 4 has the highest lift-to-drag ratio. However, as the Reynolds number increases, the CL/CD of the cavity with an aspect ratio of 4 increases while the cavity with an aspect ratio of 3 steadily declines.

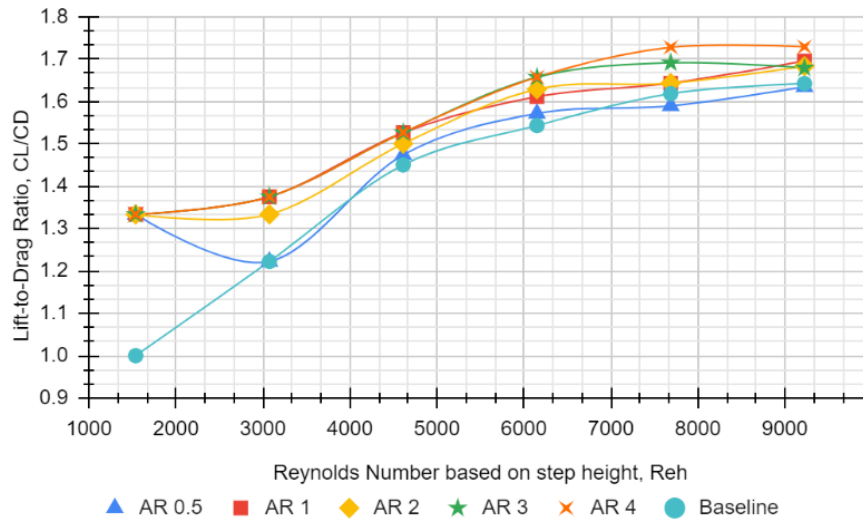


Figure 14: Graph of CL/CD vs. Reh for varying cavity aspect ratio

From here, we can conclude that the cavity with an aspect ratio of 4 has the highest aerodynamic performance compared to the others. An increase of up to 33.3% is observed at low Reynolds numbers and up to 6.7% for high Reynolds numbers. We can also conclude that while the trend observed shows that as the aspect ratio increases its aerodynamic efficiency also increases. However, its aerodynamic efficiency also depends on the aspect ratio of the cavity. From this experiment, a cavity with an aspect ratio of 4 is selected for the third experiment.

Effect of Varying Cavity Distances, d

In the third experiment, we used the cavity with an aspect ratio of 4 and tested its effectiveness at different distances from the backwards-facing steps. The distances tested were based on the height of the backwards-facing steps, h , which is 0.005m. The distances tested are 0h, 1h, 2h, 3h 4h and 5h. This experiment aims to investigate and find the correlations between the distances of the cavity from the step wall and its aerodynamic performance. From this, we could determine the best distances to use in a

WIG with a fixed aspect ratio of the cavity. Table 3 shows the parameters used in this experiment.

Table 3: Experimental parameters for varying cavity distances

Configurations	Open
Aspect Ratio, AR	4
Distance from step, d	0h (0mm)
	1h (5mm)
	2h (10mm)
	3h (15mm)
	4h (20mm)
	5h (25mm)
Ground Clearance, h/c	0.6

Figure 15 shows the line graph of lift coefficient, CL versus Reynolds number, Reh for the baseline model and different cavity distances. At first glance, it is evident that although having the same aspect ratio, the distance from the step also plays a crucial role in modifying and manipulating the flow field. Other than that, we can also see that cavity with longer distances such as 4h and 5h, has a significantly higher lift than others. However, upon closer inspection, reducing the distances from 4h to 3h and then to 2h causes a reduction in lift coefficient, CL. On the other hand, further decreasing the distances from 2h to 1h and 0h

increases the lift coefficient. This shows that placing the cavity in the middle might cause a reduction in the lift produced. Comparing the 2h and 3h cavities with the baseline model shows that there is only an improvement at a certain Reynolds number. Other cavities on the other hand, consistently generate more

lift than the baseline model. In this case, the cavity with the farthest distance, 5h, produces the highest lift with a significant increase of up to 33.3% at a low Reynolds number and up to 15% at a higher Reynolds number.

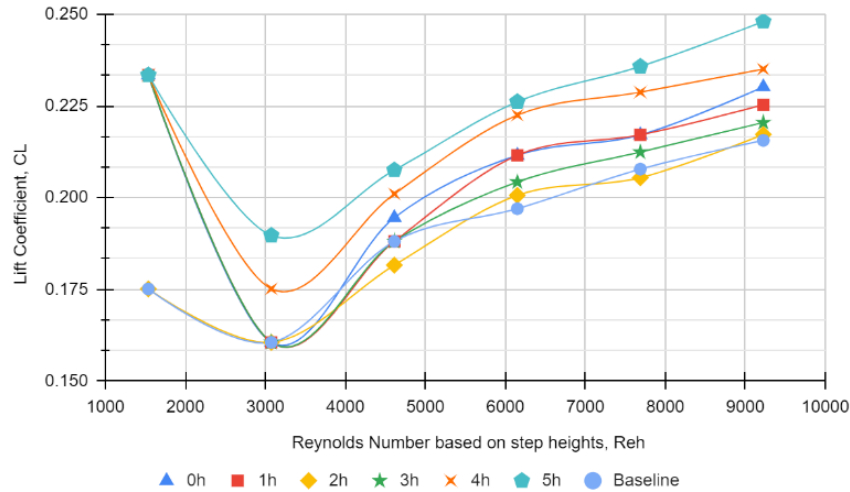


Figure 15: Graph of CL vs. Reh for varying cavity distances

Figure 16 shows the performance of different cavity distances in terms of drag coefficient, CD. From this figure, we can see that increasing the distance of the cavity from the step generally causes an increase in drag, except for the cavity with distances of 4h. The drag coefficient also significantly reduces as the cavity approaches the step wall. However, the drag coefficient increased at Reynolds number above 4000, which became higher than the baseline model. This shows that while reducing the distances can reduce

the drag produced, it is only effective for low to moderate Reynolds numbers. At a high Reynolds number, approximately above 6000, the effectiveness of the cavity in reducing the drag produced plummeted, which results in a similar drag coefficient, if not higher, compared to the baseline model. Here, the cavity which performs the best in terms of drag coefficient is 1h. This cavity can reduce the drag produced by 11% at low to moderate Reynolds numbers.

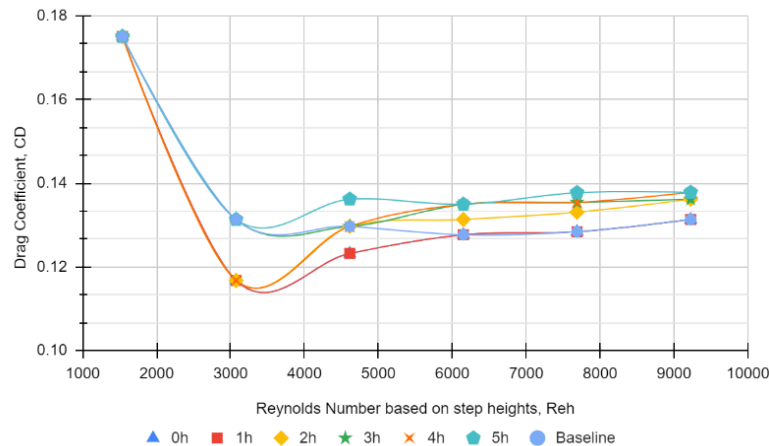


Figure 16: Graph of CD vs. Reh for varying cavity distances

Figure 17 shows the cavity's lift-to-drag ratio, CL/CD, with different distances from the step wall. From this figure, we can observe that manipulating the distances of a cavity will also affect the mean flow field behind

the backwards-facing step of the stepped hull. The graph also shows that positioning the cavity near and far from the step increases aerodynamic efficiency compared to the baseline model. Contrarily, placing

the cavity in the middle reduces aerodynamic efficiency, causing the cavity to act similarly to a baseline model. This is clearer when we refer to Figure 15 and Figure 16. Comparing these two figures, it is evident that increasing the distances of the cavity from the backward facing steps causes an increase in the lift

while reducing the distances causes a reduction in drag, placing the cavity at the middle of this range will cause the cavity to inherit the disadvantages of both regions, which makes the middle cavity becomes the worse combination for the WIG.

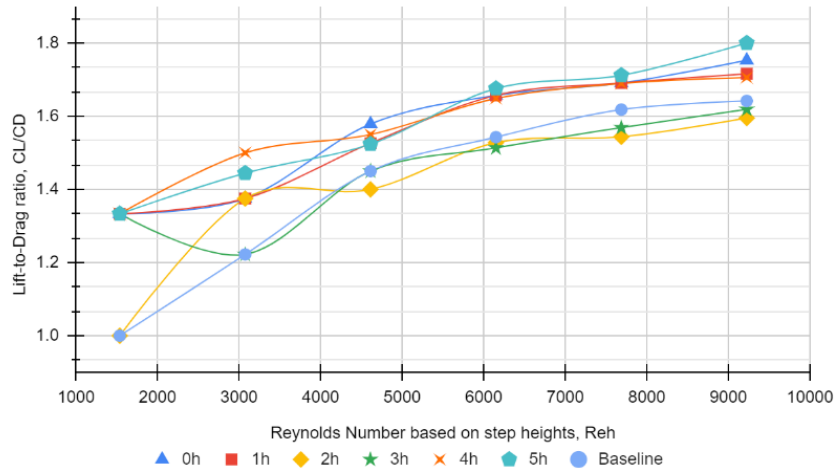


Figure 17: Graph of CL/CD vs. Reh for varying cavity distances

From Figure 17, we can also see that the performance of the different cavity distances relies on the Reynolds number. At a low Reynolds number of approximately below 4000, the cavity with distances of 4h has the highest lift-to-drag ratio. Conversely, when the Reynolds number approaches 6000, the cavity with distances of 5h has the highest lift-to-drag ratio compared to the others. From this, we can conclude that the operational Reynolds number of a WIG craft is essential to select the best distances for the cavity.

From this experiment, we find that the effectiveness of the cavity is dependent on the distances and Reynolds number. This is similar to a study conducted by Ridwan et al. [25], where they found that the location of a cavity plays a vital role in manipulating the base pressure in a convergent, divergent nozzle. Based on this study, the best

distance for a fixed aspect ratio cavity is 5h, approximately 25 mm from the step wall. An increase of up to 33.3% can be observed at low Reh and up to 9.6% at high Reynolds numbers.

Effect of Varying Ground Clearance, h/c

For the fourth experiment, the best cavity configurations, distances and aspect ratios from the previous experiment are tested at different ground clearances. This experiment aims to study the effectiveness of cavities under different flight conditions and determine the best service ceiling for a WIG craft equipped with a cavity. Table 4 shows the parameters used in this experiment.

Table 4: Experimental parameters for varying ground clearance

Configurations	Open
Aspect Ratio, AR	0.5, 1, 2, 3 & 4
Distance from step, d	5h (25mm)
Ground Clearance, h/c	0 (h = 0mm)
	0.3 (h = 22.40 mm)
	0.6 (h = 44.75 mm)
	0.9 (h = 67.12 mm)
	Out of ground

The lift coefficient graph of a cavity with an AR 4 and distance of 5h from the step wall is shown in Figure 18. It is evident from the graph that when the ground clearance is increased, the lift produced decreases. This result is common in any aircraft that utilizes the ground effect, as studied by Wiriadidjaja[3]. The

ground plane compresses the air between the aircraft and the surface, increasing lift. However, upon closer examination, it can be seen that for h/c = 0, the lift coefficient reduces dramatically. This is because, at approximately zero altitude, not enough air cushion is

produced from the ground effect, resulting in less lift being produced compared to other ground clearances.

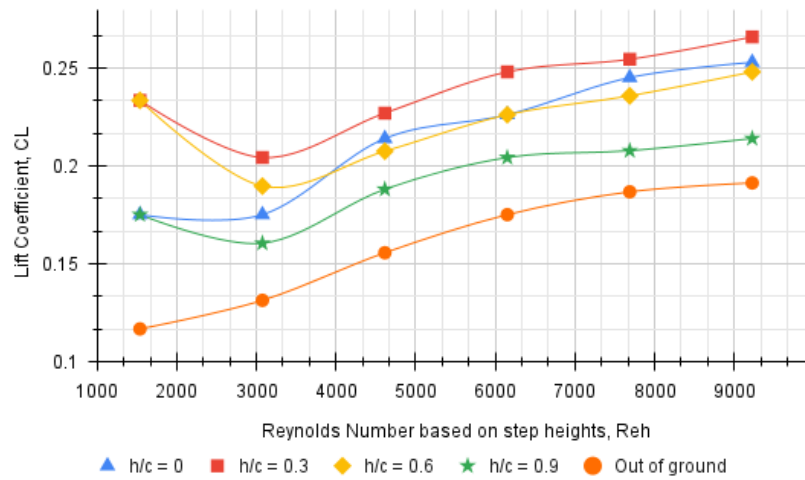


Figure 18: Graph of CL vs. Reh for varying ground clearance

Moreover, the graph in Figure 18 shows that the highest lift coefficient, CL is obtained at a ground clearance of 0.3, which is approximately 22.74 mm from the ground for all Reynolds numbers. Conversely, the lowest lift coefficient, CL, is observed when no ground plate is used and the craft is out of ground effect. At the same ground clearance of 0.3, an increase in lift of up to 7.7% is observed when compared to the baseline model tested at the same ground clearance.

The graph shown in Figure 19 shows the relationship between the drag coefficient and Reynolds number, Reh, for a WIG craft. It is evident that there is a noticeable trend between ground clearance and drag coefficients. This finding is also consistent with previous studies on normal WIGs without cavities, such as the research conducted by Wiriadidjaja [3].

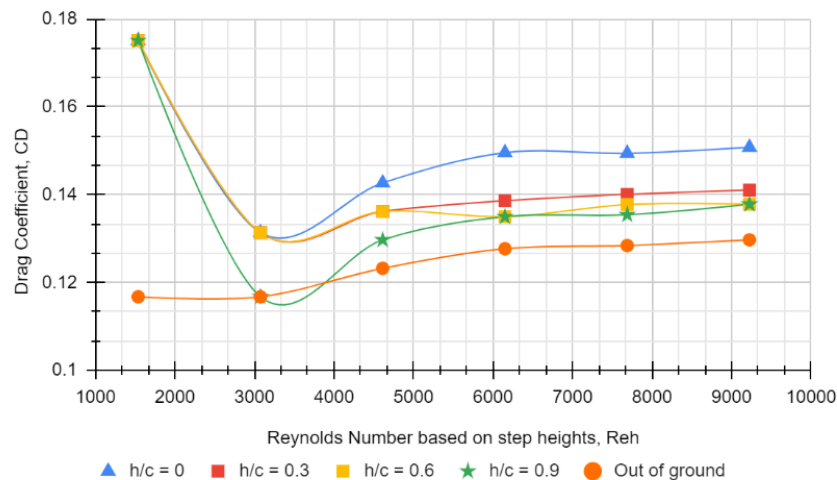


Figure 19: Graph of CD vs. Reh for varying ground clearance

Despite the increase in drag with decreasing ground clearance, the cavity performs similarly at ground clearances of 0.3, 0.6, and 0.9, with only a 2% variation. However, at ground clearance of 0, the drag coefficient increases drastically. Therefore, it is not recommended to operate a WIG craft too close to the ground as it will only nullify the advantages of ground effects.

On the other hand, the lowest drag coefficient is observed when the WIG craft is out of ground effect. This suggests that the drag produced in this experiment is a result of the ground effect itself and at a certain distance from the ground, the ground effect becomes negligible, and the drag coefficient reaches its minimum value.

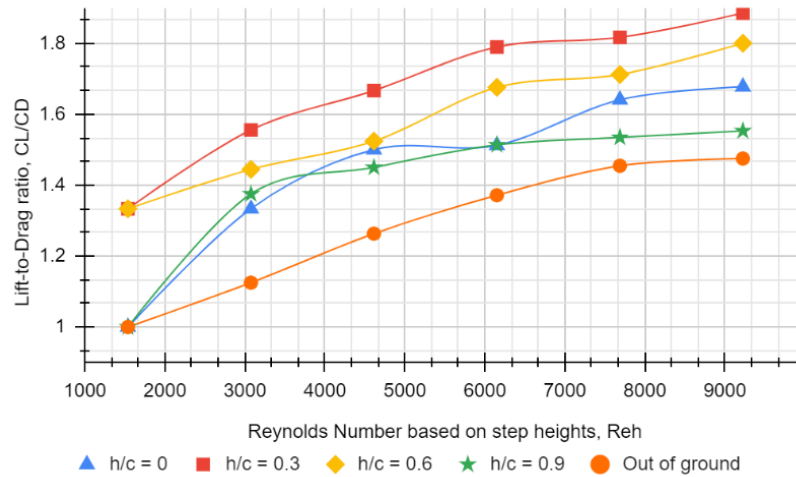


Figure 20: Graph of CL/CD vs. Reh for varying ground clearance

The lift-to-drag ratio, CL/CD, of a cavity with an aspect ratio of 4 at different ground clearance is shown in the graph in Figure 20. The figure shows that a WIG that uses a cavity will have the highest aerodynamic performance when flying or cruising at a ground clearance, h/c of 0.3. A significant improvement in CL/CD is observed at h/c of 0.3 compared to h/c of 0.6.

The trends observed in Figure 20, where the lift-to-drag ratio increases with decreasing ground clearance are also observed in a study conducted with a normal WIG craft [3]. This shows that the cavity employed in this model does not alter the nature of the ground effect and only acts as a passive controller to improve the flow field behind the backwards-facing steps of the stepped hull.

However, when the ground clearance is at its lowest point, h/c = 0, the lift-to-drag ratio of a WIG craft drops significantly compared to other ground clearances. This is because there is not enough space between the craft and the surface to create a substantial "air cushion" that would improve the lift-to-drag ratio. Consequently, it is not recommended to operate a WIG craft at such low altitudes, as the ground effect is not very efficient nor effective at this altitude, making the use of the WIG craft impractical.

According to the graph in Figure 20, the ground clearance of 0.3 provides a significant increase of up to 7% in lift-to-drag ratio when compared to the baseline model tested at the same height. This means that the cavity used plays an important role in improving the aerodynamic performance of the WIG craft with a stepped hull. However, when the craft is out of ground effect, the usage of the cavity can be considered contradictory as there is a drop of up to 1.6%. This shows that when not operating in the ground effect, the cavity acts almost similar to a closed surface or the baseline model with only a slight variation in its aerodynamic performance.

In conclusion, the WIG with a cavity is best operated at a ground clearance of 0.3 to maximise the usage of the ground effect.

CONCLUSION

In conclusion, using the cavity as a passive controller for wing-in-ground craft with a stepped hull is proven effective. Adding a cavity behind the backwards-facing step improves the craft's overall aerodynamic performance compared to the baseline model. As theorized by Rathakrishnan E. [23], the introduction of smaller secondary vortices due to the presence of a cavity helps improve the mean flow fields behind the backwards-facing step. This could result in increase in aerodynamic performance of the WIG craft for certain configurations of cavity. The best configurations found are cavity with open cavity configurations with an aspect ratio of 4 and located at 5h from the backwards-facing steps. This cavity is best employed at a ground clearance of 0.3. For this configuration, an increase of up to 7.7% in lift-to-drag ratio is observed compared to the baseline model. Further investigations on the effects of the multiple cavities, varying cavity geometry and the effectiveness of geometry at different attack angles are recommended. It is also recommended to use particle image velocimetry (PIV) to understand the flow behaviour behind the backwards-facing step with a cavity.

ACKNOWLEDGEMENT

The author would like to thank the Faculty of Engineering Universiti Pertahanan Nasional Malaysia (UPNM) for providing the necessary facilities for this study. The author would also like to express their

gratitude to all the co-authors who have contributed their expertise and involvement in this study.

References

- [1] K. V. Rozhdestvensky, "Wing-in-ground effect vehicles," *Progress in aerospace sciences*, vol. 42, no. 3, pp. 211–283, 2006.
- [2] Erjie Cui and Xin Zhang. Ground effect aerodynamics. *Encyclopedia of Aerospace Engineering*, 1(Part 3):245–256, 2010.
- [3] Surjatin Wiriadidjaja, Amzari Zhahir, Zahratu Hilal Mohamad, Shikin Razali, Ahmad Afifi Puaat, and Mohamed Tarmizi Ahmad. Wing-in-ground-effect craft: A case study in aerodynamics. *International Journal of Engineering & Technology*, 7(4):5–9, 2018.
- [4] NA Ahmed and J Goonaratne. Lift augmentation of a low-aspect-ratio thick wing in ground effect. *Journal of Aircraft*, 39(2):381–384, 2002.
- [5] E. I. A. Amin, "Efficiency of wing-in-ground marine crafts," Department of Naval Architecture and Marine Engineering Faculty of Engineering Port Said University, 2011.
- [6] Kirill V Rozhdestvensky. Aerodynamics of a lifting system in extreme ground effect. Springer Science & Business Media, 2000.
- [7] Koe Han Beng. On the hydrodynamics of stepped hull. PhD thesis, National University of Singapore (Singapore), 2016.
- [8] N. Saputra, M. M. B. Tofa, I. Suharyanti, and S. Jamei, "Effect Of Stepped Hull On Wing In Ground Effect (WIG) Craft During Take Off," in *3rd International Graduate Conference on Engineering, Science and Humanities (IGCESH)*, School of Graduate Studies Universiti Teknologi Malaysia, 2010.
- [9] Lin Chen, Keisuke Asai, Taku Nonomura, Guannan Xi, and Tianshu Liu. A review of backward-facing step (bfs) flow mechanisms, heat transfer and control. *Thermal Science and Engineering Progress*, 6:194–216, 2018.
- [10] Dwarikanath Ratha and Arindam Sarkar. Analysis of flow over backward facing step with transition. *Frontiers of Structural and Civil Engineering*, 9:71–81, 2015.
- [11] P Sujar-Garrido, N Benard, E Moreau, and JP Bonnet. Dielectric barrier discharge plasma actuator to control turbulent flow downstream of a backward-facing step. *Experiments in Fluids*, 56:1–16, 2015.
- [12] Sohrab Gholamhosein Pouryoussefi, Masoud Mirzaei, and Majid Hajipour. Experimental study of separation bubble control behind a backward-facing step using plasma actuators. *Acta Mechanica*, 226:1153–1165, 2015.
- [13] Khuder N Abed. Flow separation control of backward-facing step airfoil naca0015 by blowing technique. *Diyala Journal of Engineering Sciences*, pages 99–119, 2019.
- [14] Mansop Hahn and W Pfenninger. Prevention of transition over a backward step by suction. *Journal of Aircraft*, 10(10):618–622, 1973.
- [15] Istvan Bolgar, Sven Scharnowski, and Christian J Kähler. Control of the reattachment length of a transonic 2d backward-facing step flow. In *Proceedings of the 5th International Conference on Jets, Wakes and Separated Flows (ICJWSF2015)*, pages 241–248. Springer, 2016.
- [16] Zinnyrah Methal, Ahmad Syahin Abu Talib, Mohd Supian Abu Bakar, Mohd Rosdzimin Abdul Rahman, Mohamad Syafiq Sulaiman, and Mohd Rashdan Saad. Improving the aerodynamic performance of wig aircraft with a micro-vortex generator (mvg) in low-speed condition. *Aerospace*, 10(7):617, 2023.
- [17] AAT Syahin, M Zinnyrah, NA Azfar, I Said, A Che Idris, MRA Rahman, and MR Saad. Effect of micro-ramp vortex generator in improving aerodynamics performance of wing-in-ground craft fuselage. *Perintis eJournal*, 11(1):61–69, 2021.
- [18] Irahasira Said, Mohd Rosdzimin Abdul Rahman, Azam Che Idris, Fadhilah Mohd Sakri, and Mohd Rashdan Saad. The effect of flow control on wing-in-ground craft hull-fuselage for improved aerodynamics performance. In *Proceedings of International Conference of Aerospace and Mechanical Engineering 2019: AeroMech 2019*, 20–21 November 2019, Universiti Sains Malaysia, Malaysia, pages 501–510. Springer, 2020.
- [19] Vigneshvaran Sethuraman, Parvathy Rajendran, and Sher Afghan Khan. Base and wall pressure control using cavities and ribs in suddenly expanded flows-an overview. *Journal of Advanced Research in Fluid Mechanics and Thermal Sciences*, 66(1):120–134, 2020.
- [20] Sher Afghan Khan, Abdulrahman Abdulla Al Robaian, Mohammed Asadullah, and Abdul Mohsin Khan. Grooved cavity as a passive controller behind backward facing step. *Journal of Advanced Research in Fluid Mechanics and Thermal Sciences*, 53(2):185–193, 2019.
- [21] Sher Afghan Khan, Mohammed Asadullah, GM Fharukh Ahmed, Ahmed Jalaluddeen, and Maughal Ahmed Ali Baig. Passive control of base drag in compressible subsonic flow using multiple cavity. *Int. J. Mech. Prod. Eng. Res. Dev*, 8(4):39–44, 2018.
- [22] KM Pandey and E Rathakrishnan. Annular cavities for base flow control. *International Journal of Turbo and Jet Engines*, 23(2):113–128, 2006.
- [23] E Rathakrishnan, OV Ramanaraju, and K Padmanaban. Influence of cavities on suddenly expanded flow field. *Mechanics research communications*, 16(3):139–146, 1989.
- [24] Krishna Murari Pandey and E Rathakrishnan. Influence of cavities on flow development in sudden expansion. *International Journal of Turbo and Jet Engines*, 23(2):97–112, 2006.
- [25] Ridwan, N. H. M. Zuraidi, I. M. Shaikh, and S. A. Khan, "Passive Control of Base Pressure Using Cavities in A Sudden Expansion Duct: A CFD Approach," *Journal of Mechanical Engineering Research and Developments*, vol. 45, no. 3, pp. 44–70, Jun. 2022